

Proposal:	5-31-2227	Council:	4/2012
Title:	The interplay between magnetism and superconductivity in $\text{Ho}(\text{Ni}_{1-x}\text{Co}_x)_2\text{B}_2\text{C}$ ($x=0, 0.2, \dots, 1$): probing the evolution of magnetic modes		
This proposal is a new proposal			
Research Area:	Physics		

Main proposer: EL MASSALAMI Mohammed

Experimental Team: EL MASSALAMI Mohammed

Local Contact: OULADDIAF Bachir

Samples: $\text{Ho}(\text{Co}_x\text{Ni}_{1-x})_2\text{B}_2\text{C}$ [$x=0, 0.2, 0.4, 0.6, 0.8, 1$]

Instrument	Req. Days	All. Days	From	To
D2B	3	3	16/11/2012	19/11/2012

Abstract:

Recently we observed a cascade of magnetic modes in $\text{Tb}(\text{Co}_x\text{Ni}_{1-x})_2\text{B}_2\text{C}$: from a LSDW $k = (0.55, 0, 0)$ state at $x = 0$, to a collinear $k = (0.5, 0, 0.5)$ AFM state at $x = 0.2, 0.4$; then a transverse c axis modulated $k = (0, 0, 1/3)$ mode at $x = 0.6$, and finally a simple FM mode at $x = 0.8, 1$. The observation of the $k = (0, 0, 1/3)$ mode, which has not been observed before in borocarbides, confirms the prediction by Rhee et al. [PRB51,15585(1995)] of a peak in the generalized susceptibility. Although this model explains the surge of this mode, however it fails to explain the surge of the other modes: this is most probably due to dis-consideration of the interplay between superconductivity (SUP) and magnetism (MAG). Such an approach was undertaken by Bertussi et al [PRB79,220513(2009)] who did predict a co-existence of SUP and MAG and also the surge of a cascade of magnetic modes if MAG and SUP couplings are properly tuned. In fact $\text{Tb}(\text{CoNi})_2\text{B}_2\text{C}$ can be considered as non-SUP limit of their phase diagram. To explore fully this model we proposed to investigate this interplay in $\text{Ho}(\text{Co}_x\text{Ni}_{1-x})_2\text{B}_2\text{C}$ wherein $x=0$ ($x=1$) is a AFM SUP (normal FM). Does the modes of this series verify the predicted phase diagram?

HoNi₂B₂C is a model system wherein magnetism, superconductivity and their interplay are manifested:^{1,2} it superconducts at $T_c \approx 8.5$ K and, well below T_c , it exhibits two incommensurate AFM modes around $T_m \approx 6$ K and these are replaced by an AFM state below $T_N \approx 5$ K (see Table I). Within $T_N < T < T_m$, a reentrant behavior of $H_{c2}(T)$ emerges testifying to the strong coupling between magnetism and superconductivity. The influence of chemical substitution on such a rich manifestation of magnetism, superconductivity and their interplay had been extensively probed in, e.g., Ho(Co_xNi_{1-x})₂B₂C ($0 \leq x \leq 1$):^{3,4} superconductivity is steeply suppressed (see Fig. 1(b)), nonetheless, the parent magnetic modes are hardly influenced at low x . Obviously, such a mode stability is not expected for higher Co substitution (indeed the magnetic structure of HoCo₂B₂C is FM⁵). The question is how does the magnetic structure evolve with substitution, going from AFM mode at $x = 0$ to FM at $x = 1$. This work investigated the evolution of the magnetism (in particular the magnetic structure with their distinct \vec{k}^x , μ_{sat}^x , T_{cr}^x) of Ho(Co_xNi_{1-x})₂B₂C ($0 \leq x \leq 1$).

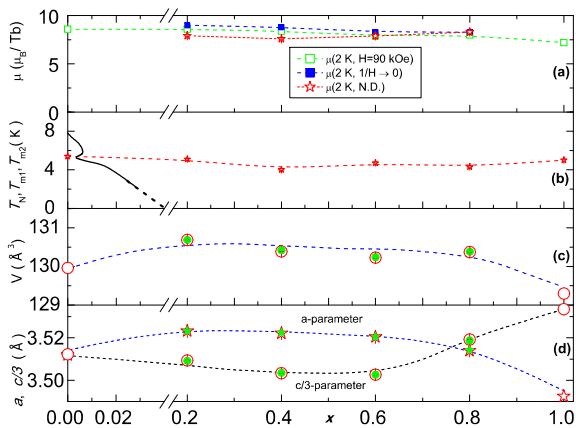


FIG. 1. Some properties of Ho(Ni_{1-x}Co_x)₂B₂C plotted as function of x . The dashed lines are guide to the eye. (a) Magnetic moment as obtained from neutron diffraction (stars), $\mu(2\text{ K}, 90\text{ kOe})$ (open squares), and $\mu(2\text{ K}, 1/H \rightarrow 0)$ (filled squares). (b) Magnetic transition temperatures as determined from the magnetic susceptibility and specific heat (data of $x=0$ are taken from Refs. 1 and 2 while that of $x=1$ from Ref. 5). The solid line represents the superconducting transition temperature as reported in Ref. 3. (c) Unit-cell volume measured at 2 K (open circles) and 30 K (solid circles); (d) measured unit-cell a parameter at 2 K (open stars) and 30 K (solid stars); $c/3$ parameter at 2 K (open circle) and 30 K (solid circle).

Powder neutron-diffractograms were collected at the high resolution powder diffractometer D2B ($\lambda = 1.6\text{\AA}$, $T = 1.5\text{K}$ and 30K). Rietveld analysis of the neutron diffractograms taken above T_{cr}^x [see Fig. 3 (a-d)] indicate an almost single-phase tetragonal $I4/mmm$ crystal structure. The lattice parameters, Fig. 1(c-d), evolve smoothly but non-monotonically with the Co concen-

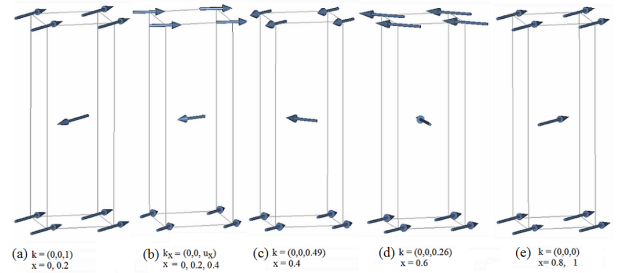


FIG. 2. The 1.5 K magnetic structures of the studied Ho(Co_xNi_{1-x})₂B₂C compositions. For completeness, we also include the contaminating spiral modes of $x=0.2, 0.4$ (see text).

tration. On lowering the temperature down to 1.5 K, the same tetragonal crystal structure is maintained for all studied compositions (i.e. no orthorhombic distortion within available accuracy). Evidently, anisotropic magnetoelastic forces are much weaker than the ones observed in, say, isomorphous Tb(Co_xNi_{1-x})₂B₂C.⁷⁻⁹

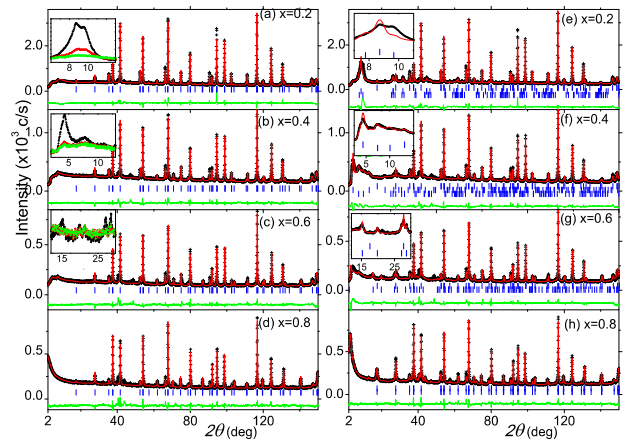


FIG. 3. (Color online) Neutron diffractograms of Ho(Ni_xCo_{1-x})₂B₂C, measured at (a-d) $T = 30$ K showing the tetragonal crystal structure, and (e-h) at $T = 1.5$ K showing additional magnetic contribution. *Insets* (a-c): Difference plots showing the thermal evolution of the magnetic contribution: $I(1.5\text{ K}) - I(30\text{ K})$ (black), $I(3\text{ K}) - I(30\text{ K})$ (red), and $I(6\text{ K}) - I(30\text{ K})$ (green). *Insets* (e-g): an expansion showing the lower peaks of the involved magnetic modes. Space groups, positions, occupations, thermal parameters are similar to those reported by Lynn *et al.*⁶ $\vec{\mu}_{ND}$ and lattice parameters are given in Fig. 1, while \vec{k}^x in Fig. 2.

The magnetic modes which are evident in Fig. 3 can be readily identified:

a. Ho(Co_{0.2}Ni_{0.8})₂B₂C: The main magnetic mode of Fig. 3 (e) is a commensurate AF structure with $\vec{k}_1^{x=0.2} = (0, 0, 1)$ and $\mu_{ND}^{x=0.2} = 8.7(1)\mu_B$. This mode is the same as the one observed in the $x = 0$ case and as such the easy axis is assumed to be along $(1, 1, 0)$.⁶ A careful look at Fig. 3 (e) reveals additional (but weak) magnetic peaks; the most evident ones are shown in

TABLE I. Selected magnetic properties of $\text{Ho}(\text{Co}_x\text{Ni}_{1-x})_2\text{B}_2\text{C}$. For studied samples, μ_{ND} is moment as obtained from neutron diffraction while μ_{M} is the saturated, $1/H \rightarrow 0$, moment as obtained from magnetization isotherms. Moments are confined to the ab planes (see text). For completeness, the contaminating spiral modes at $x=0.2$ and 0.4 are included. Data for $x=0$ are taken from Refs.6 while that of $x=1$ from Ref.5.

x	0	0.2	0.4	0.6	0.8	1.0			
structure	AFM	Spiral	AFM	Spiral	Spiral	Spiral	FM	FM	
\vec{k}^x	(0, 0, 1)	(0,0,0.92)	(0, 0, 1)	(0, 0, 0.85)	(0, 0, 0.49)	(0, 0, 0.89)	(0, 0, 26)	(0, 0, 0)	(0, 0, 0)
$ \vec{\mu} _{\text{ND}} (\mu_B)$	8.6	6.7	8.7	4.8(2)	5.3	5.2	7.4(2)	8.3	7.2
$ \vec{\mu} _{\text{M}} (\mu_B)$	8.6		9.0		8.8		8.3	8.3	7.2

the inset of Fig. 3 (e). These pertain to an incommensurate c -axis spiral $\vec{k}_2^{x=0.2} = (0, 0, 0.85)$ mode with $\mu_1^{x=0.4}=4.8(2) \mu_B$ (each consecutive FM plane is rotated by 153.7°); this mode is similar to the $\vec{k}_2^{x=0} = (0, 0, 0.92)$ mode observed in $\text{HoNi}_2\text{B}_2\text{C}$ within the range $5 < T < 8.5$ K (Ref. 6) and in $\text{Ho}(\text{Co}_x\text{Ni}_{1-x})_2\text{B}_2\text{C}$ ($x \leq 0.015$).⁴ As the strength of this mode is extremely weak and furthermore it is also present as a minority mode in the $x=0.4$ composition, then it is taken to be due to magnetic contamination.

b. $\text{Ho}(\text{Co}_{0.4}\text{Ni}_{0.6})_2\text{B}_2\text{C}$: Figure 3 (f) indicates that the main magnetic contribution is an incommensurate c -axis spiral modes with $\vec{k}_1^{x=0.4} = (0, 0, 0.49)$ and $\mu_1^{x=0.4}=5.3 \mu_B$ (the FM planes along the c -axis are rotated by almost 90°). There is an additional weak $\vec{k}_2^{x=0.4} = (0, 0, 0.89)$ mode with $\mu_1^{x=0.4} = 5.2 \mu_B$ (the spiral rotation angle is 161°): as discussed above in the $x = 0.2$ case, it is taken to be due to a contaminating phase.

c. $\text{Ho}(\text{Co}_{0.6}\text{Ni}_{0.4})_2\text{B}_2\text{C}$: The magnetic order, shown in Fig. 3 (g), consists of a single incommensurate mode with $\vec{k}_1^{x=0.6} = (0, 0, 0.26)$ (the FM planes are rotated by 46.8°) and $\mu_{\text{sat}}^{x=0.6}=7.4(2)\mu_B$.

d. $\text{Ho}(\text{Co}_{0.8}\text{Ni}_{0.2})_2\text{B}_2\text{C}$: The magnetic structure, Fig. 3 (h), consists of a single FM $\vec{k}_1^{x=0.8} = (0, 0, 0)$ mode with $\mu_{\text{sat}}^{x=0.8}=8.3(2)\mu_B$: this magnetic structure is similar to the one observed in $\text{HoCo}_2\text{B}_2\text{C}$ wherein $\mu_{\text{sat}}^{x=1}=7.6(2)\mu_B$.⁵

A variation in Co substitution (or temperature) is expected to modify the detail of the electronic structure which in turn influences the generalized susceptibilities, $\chi(q)$, and as such leads to the observed cascade of magnetic modes. Specifically, the energetically favorable magnetic mode is the one wherein $\chi(q)$ [or $J(q)$ since $J(q) \propto I^2 \cdot \chi(q)$] reaches a maxima. For borocarbides, the calculated normal-state $\chi(q)$ function, along the c^* axis, does reveal local maximas, e.g., at $\vec{k}_{\text{cal}} = (0, 0, 0.3)$ and $\vec{k}_{\text{cal}} = (0, 0, 0.9)$.¹⁰ these vectors have been observed before.^{6,8} One of the main result of this work is the revelation that such a wave vector can be controlled by Co substitution: variation in x of $\text{Ho}(\text{Co}_x\text{Ni}_{1-x})_2\text{B}_2\text{C}$ modifies u^x of $\vec{k}^x = (0, 0, u^x)$. It is recalled that a simplified molecular field approach indicates that $T_{\text{cr}} \propto J(q)$; accordingly, the observation that $T_{\text{cr}}^x \sim 5$ K for all compositions indicates that though the position of $J(q)$ (or $\chi(q)$) shifts with x but its value (thus T_{cr}^x) is hardly modified.

The ease with which these wave vectors can be modified by temperature or electron count variation suggests that the exchange couplings are much stronger than the CEF forces which, if dominant, would tend to pin the R moments along the equivalent easy axes. Then the results on $\text{Ho}(\text{Co}_x\text{Ni}_{1-x})_2\text{B}_2\text{C}$ ($0 \leq x \leq 1$) (as well as that on $\text{Tb}(\text{Co}_x\text{Ni}_{1-x})_2\text{B}_2\text{C}$ ($0.4 < x \leq 1$))⁸ indicate that all these widely different magnetic modes are nothing but a variation on the stacking sequence of the individual FM R sheets: see Fig. 2 wherein moments orientation along the z -axis is described by $\vec{S}_n = S \cdot (\cos(\vec{k}^x \cdot \vec{r}_n), \sin(\vec{k}^x \cdot \vec{r}_n), 0)$.

¹ K.-H. Müller and V. N. Narozhnyi, Rep. Prog. Phys. **64**, 943 (2001).

² L. C. Gupta, Adv. Phys. **55**, 691 (2006).

³ H. Schmidt and H. F. Braun, Phys. Rev. B **55**, 8497 (1997).

⁴ J. W. Lynn, Q. Huang, A. Santoro, R. J. Cava, J. J. Krajewski, and W. F. Peck, Phys. Rev. B **53**, 802 (1996).

⁵ M. ElMassalami, R. Moreno, H. Takeya, B. Ouladdiaf, J. W. Lynn, and R. S. Freitas, J. Phys: Condens Matter **21**, 436006 (2009).

⁶ J. W. Lynn, S. Skanthakumar, Q. Huang, S. K. Sinha, Z. Hossain, L. C. Gupta, R. Nagarajan, and C. Godart, Phys. Rev. B **55**, 6584 (1997).

⁷ M. ElMassalami, R. Moreno, R. M. Saeed, F. A. B. Chaves, C. M. Chaves, R. E. Rapp, H. Takeya, B. Ouladdiaf, and M. Amara, J. Phys: Condens Matter **21**, 216006 (2009).

⁸ M. ElMassalami, H. Takeya, B. Ouladdiaf, R. Maia Filho, A. M. Gomes, T. Paiva, and R. R. dos Santos, Phys. Rev. B **85**, 174412 (2012).

⁹ M. ElMassalami, A. Gomes, T. Paiva, R. dos Santos, and H. Takeya, Journal of Magnetism and Magnetic Materials **335**, 163 (2013).

¹⁰ J. Y. Rhee, X. Wang, and B. N. Harmon, Phys. Rev. B **51**, 15585 (1995).